re-B

You have downloaded a document from
RE-BUŚ
repository of the University of Silesia in Katowice

Title: Synthetic strategy matters : the study of a different kind of PVP as micellar vehicles of metronidazole

Author: Rafał Bielas, Paulina Maksym, Magdalena Tarnacka, Karolina Jurkiewicz, Agnieszka Talik, Monika Geppert-Rybczyńska, Joanna Grelska, Roksana Bernat, Kamil Kamiński, Marian Paluch i in.

Citation style: Bielas Rafał, Maksym Paulina, Tarnacka Magdalena, Jurkiewicz Karolina, Talik Agnieszka, Geppert-Rybczyńska Monika, Grelska Joanna, Bernat Roksana, Kamiński Kamil, Paluch Marian i in. (2021). Synthetic strategy matters : the study of a different kind of PVP as micellar vehicles of metronidazole. "Journal of Molecular Liquids" (Vol. 332 (2021), art. no. 115789), doi 10.1016/j.molliq.2021.115789

Uznanie autorstwa - Użycie niekomercyjne - Bez utworów zależnych Polska - Licencja ta zezwala na rozpowszechnianie, przedstawianie i wykonywanie utworu jedynie w celach niekomercyjnych oraz pod warunkiem zachowania go w oryginalnej postaci (nie tworzenia utworów zależnych).

UNIWERSYTET ŚLĄSKI W KATOWICACH
Biblioteka Uniwersytetu Śląskiego
Ministerstwo Nauki i Szkolnictwa Wyższego

Journal of Molecular Liquids 332 (2021) 115789

Contents lists available at ScienceDirect

Journal of Molecular Liquids

journal homepage: www.elsevier.com/locate/molliq

Synthetic strategy matters: The study of a different kind of PVP as micellar vehicles of metronidazole

Rafał Bielas [a,c,*], Paulina Maksym [a,c,*], Magdalena Tarnacka [a,c], Aldona Minecka [d], Karolina Jurkiewicz [a,c], Agnieszka Talik [a,c], Monika Geppert-Rybczyńska [a,b], Joanna Grelska [a,c], Łukasz Mielańczyk [e], Roksana Bernat [a,c], Kamil Kamiński [a,c,*], Marian Paluch [a,c], Ewa Kamińska [d]

[a] Chelkowski Institute of Physics, University of Silesia in Katowice, 75 Pułku Piechoty 1, 41-500 Chorzów, Poland
[b] Institute of Chemistry, University of Silesia, Szkolna 9, 40-006 Katowice, Poland
[c] Silesian Center for Education and Interdisciplinary Research, University of Silesia, ul. 75 Pulku Piechoty 1A, 41-500 Chorzow, Poland
[d] Department of Pharmacognosy and Phytochemistry, Faculty of Pharmaceutical Sciences in Sosnowiec, Medical University of Silesia in Katowice, ul. Jagiellońska 4, 41-200 Sosnowiec, Poland
[e] Department of Histology and Cell Pathology, Faculty of Medical Sciences in Zabrze, Medical University of Silesia, 40-055 Katowice, Poland

ARTICLE INFO

Article history:
Received 15 January 2021
Accepted 25 February 2021
Available online 01 March 2021

Keywords:
Metronidazole
Poly(1-vinyl-2-pyrrolidone)
Drug delivery
Drug delivery systems
Micelles

ABSTRACT

Poly(1-vinyl-2-pyrrolidone) (Povidone, PVP) is one of the most interesting and versatile synthetic polymers utilised in the pharmaceutical and cosmetic industries. Its large-scale commercial production offers an assortment of products in a wide range of molecular weights but poorly-controlled (macro)structural parameters (i.e., dispersity, functionality) limiting the efficiency of PVP-based drug delivery systems (DDS). In this work, synthesised linear and star-shaped PVPs with a strictly defined structure and functionality were compared with the linear, commercially-supplied product and explored as potential vehicles for physical entrapment of metronidazole (MTZ). Here, a question is addressed how differences in their macromolecular properties affect the amorphisation of MTZ, drug encapsulation, the stability of drug-loaded micellar structures and their in vitro release from the carrier. The X-ray diffraction studies and calorimetric measurements revealed that MTZ crystallises in all investigated herein systems reducing the glass transition temperature of the binary mixture significantly. Transmission electron microscopy and dynamic light scattering analysis revealed that MTZ-loaded DDS are able to form ultrasmall regular nanocarriers with an increasing effect of regularity and sphericity from star-shaped DDS to linear-based ones. We founded that synthesised linear-based DDS is the most effective for MTZ entrapment (PVP:MTZ = 1:1 weight ratio) due to their smallest hydrodynamic radius d_h = 14.7 nm, the highest stability of micellar structures −2.37 mV, and the highest values of loaded drug 76.5%. Moreover, all applied PVP-based DDS revealed an initial burst release effect of MTZ (pH = 7.4) reaching up to 60% of drug released within the first 5 h (the first-order release model fits). The marked efficiency of MTZ-loaded DDS of strictly defined structural parameters indicates the great importance of polymer preparation strategy in the targeted therapy.

© 2021 The Author(s). Published by Elsevier B.V. This is an open access article under the CC BY-NC-ND license (http://creativecommons.org/licenses/by-nc-nd/4.0/).

1. Introduction

Polymeric materials have received increasing attention as new additives for drug formulations and drug delivery systems (DDS) [1,2]. The most desirable are non-toxic, biocompatible/biodegradable macromolecules of tailor-made parameters (i.e., those characterised by targeted molecular weight, M_n, low molecular weight distribution – Đ dispersity, preserved chain-end fidelity) produced via various kinds of controlled radical polymerisation methods (CRP). Due to their unique properties, polymeric vehicles can modify the way the drug is solubilised, distributed and transported into the organism. In fact, there are many different ways of using polymers to enhance drug bioavailability [3]. The most common ones include preparation of physical mixtures or solid dispersions that affects the degree of crystallinity, physical state, and thermodynamic properties of active pharmaceutical ingredients (APIs) leading in consequence to the improvement of their pharmacokinetic parameters [4]. Recently, micellar/microspherical polymeric (nano)carriers attracted special attention, since they not only enable the encapsulation of poorly soluble hydrophobic substances what increases their bioavailability but also affects API's release at specific molecular targets. Noteworthy, by a simple modification of the composition and topology of polymeric matrices, it is possible to design DDS for long-term drug release [5,6].

* Corresponding authors at: Chelkowski Institute of Physics, University of Silesia in Katowice, 75 Pułku Piechoty 1, 41-500 Chorzów, Poland.
E-mail addresses: rafal.bielas@smcebi.edu.pl (R. Bielas), paulina.maksym@smcebi.edu.pl (P. Maksym), kamil.kaminski@smcebi.edu.pl (K. Kamiński).

https://doi.org/10.1016/j.molliq.2021.115789
0167-7322/© 2021 The Author(s). Published by Elsevier B.V. This is an open access article under the CC BY-NC-ND license (http://creativecommons.org/licenses/by-nc-nd/4.0/).

Despite the enormous progress in this field, there is still large room for improvement for micellar-based formulations that in majority cases do not bring satisfactory therapeutic effects. As a consequence, the modification of existing solutions and designing novel ones are of key importance in pharmaceutical and biochemistry scientific/industrial fields. In this way, a change of both, forms of drugs (i.e., production of salts/esters, amorphisation) and polymeric matrices (composition, topology), has been systematically investigated [7]. Notably, searching for more efficient DDS, providing a faster dissolution and enhanced bioavailability, is particularly important for APIs that to date have formed only a few devices to sustainably drug delivery. One of them is metronidazole (MTZ) gaining interest due to its great antibacterial activity, especially because of its use as a medicine for a lifestyle disease, such as gastric ulcers caused by the infection with *H. pylori*. It needs to be emphasised that some of the few attempts of MTZ releasing DDS consisted of chitosan [8], silica/polydimethylsiloxane/calcium xerogels [9], Eudargit-carrageenan mixtures [10], or even hydrogels based on crosslinked polymethacrylates [11] and poly(1-vinyl-2-pyrrolidone) (PVP) [12]. An interesting solution seems to be the use of polymer microspheres, which ensure gastric retention of the drug and, additionally, slow down its release due to the necessity of prior degradation of the carrier. Among this type of drug delivery systems, some attempts have been made with the use of alginate [13] or chitosan and esterified cellulose mixtures [14].

Inspired by these strategies, here we proposed and developed another kind of drug carriers based on polymeric micelles, and demonstrated it as an efficient vehicle for MTZ. As a model polymeric matrix, PVP, approved for the internal use by the Food and Drug Administration (FDA) [15] has been selected. Note that due to its widespread commercial availability, many different applications were found for this polymer as a drug carrier, starting from electrospun, drug-coated dressings for transdermal delivery [16–18], bioconjugates with different APIs [19,20] or peptides [21], nanostructured API-polymer composites [22] ending to hydrogels with chitosan [23] or pectin [24]. Interestingly, despite such a huge and increasing demand for PVP, its large-scale synthesis upon uncontrolled polymerisation allows the production of poorly defined macromolecules (lack of control over M_n and Đ). Although significant progress has been made on a laboratory scale due to the use of CRP methods to 1-vinyl-2-pyrrolidone (VP) polymerisation (mainly the reversible addition-fragmentation chain transfer, RAFT), the synthesis of the well-defined linear and star-shaped PVP of $M_n > 40$ kg/mol remains a challenge for modern macromolecular science or industry [25,26]. Interestingly, the implementation of the methodology based on high-pressure (HP) offered a unique opportunity to reduce/eliminate limitations of ambient-pressure strategies, making it possible to obtain higher molecular weight PVP of linear and star-shaped topology, characterised by much better structural parameters than the commercial material [27,28].

Here, having the well-defined linear and four-arm star-shaped PVP produced via 'green' catalyst- and solvent-free HP strategies, we set out to check, whether the matrix topology can influence the ability to drug encapsulation (leading to API's amorphisation), the stability of drug-loaded structures, and ability to effectively release the drug from the carrier. Another aspect worth investigating is the difference in the ability to solubilize the drug, and its releasing between two linear matrices obtained by different polymerisation strategies (controlled, solvent-free vs commonly used uncontrolled solvent-assisted). Investigated herein micellar DDS were prepared via solvent evaporation method using different PVP-MTZ weight ratios. Differential scanning calorimetry (DSC) and X-ray diffraction (XRD) measurements were carried out to characterise the thermal and structural properties of the produced formulations. Size and self-assembly of obtained DDS were examined using dynamic light scattering (DLS) and transmission electron microscopy (TEM). The drug loading content (DLC) and drug release studies (in phosphate buffer solution pH = 7.4) were performed through UV-VIS spectroscopy.

2. Materials and methods

Commercially available poly(1-vinyl-2-pyrrolidone) K90, Dulbecco's phosphate-buffered saline (modified, without calcium chloride and magnesium chloride) were purchased from Sigma Aldrich. Methanol was obtained from Chempur. MTZ was bought from Sigma-Aldrich. Linear and star-shaped PVPs were obtained according to the previously described method [28,29].

2.1. Drug loading and micelle preparation

PVPs and MTZ were dissolved in methylene dichloride CH_2Cl_2 (or chloroform, depending on polymeric matrix solubility) with the following polymer/drug weight ratios: 2:1, 1:1 and 1:2 similarly to previously reported procedures [30–36]. Solutions were added dropwise into deionised water and stirred overnight to evaporate the organic solvent. An excess of not encapsulated drug was removed via filtration (following by the use of syringe filters). Next, aqueous solutions were lyophilised. The absence of organic solvent in both empty and drug-loaded micelles was confirmed via NMR and FT-IR analysis (please see Supplementary Information). DLC was calculated from the following equation: $DLC = \frac{m_{DM}}{m_{DLM}} \times 100\%$, where m_{DM} is the amount of drug in micelles, while m_{DLM}- the amount of drug-loaded micelles.

2.2. Drug release studies

Polymer-drug systems (2 mg) were dissolved in Phosphate-buffered saline (PBS) pH = 7.4 (1.0 mL). The solution was introduced into a dialysis cellulose membrane bag (MWCO 3.5 kDa), which was placed into a glass vial with 30 mL of PBS and stirred at 37 °C in a water bath. The dialysis was carried out for 30 h. The buffer solution samples (100 μL) were taken from the release medium at appropriate time intervals and dissolved in methanol (1 mL) to determine the concentration of released drug by UV–Vis spectroscopy.

2.3. Gel permeation chromatography

Molecular weights (M_n) and dispersity indices (Đ) were determined by size-exclusion chromatography (SEC, Agilent Technologies, Santa Clara, CA, USA) equipped with an 1100 Agilent 1260 Infinity isocratic pump, autosampler, degasser, thermostatic box for columns, and differential refractometer MDS RI Detector. Addon Rev. B.01.02 data analysis software (Agilent Technologies, Santa Clara, CA, USA) was used for data collecting and processing. The SEC calculated molecular weights were based on calibration applying linear polystyrene standards (Mp = 580–1,390,000 g/mol). Pre-column guard 5 μm (50 × 7.5 mm) and two columns: PLGel 5 μm MIXED-C (300 × 7.5 mm) and Malvern Visocotek T6000M (300 × 8 mm) were used for separation. The measurements were carried out in DMF (HPLC grade) as the eluent containing 10 mM LiBr, at $T = 40$ °C with a flow rate of 0.8 mL/min.

2.4. Differential scanning calorimetry

Calorimetric measurements were carried out by using a Mettler-Toledo DSC apparatus equipped with a liquid nitrogen cooling accessory and an HSS8 ceramic sensor (heat flux sensor with 120 thermocouples). Temperature and enthalpy calibrations were performed by using indium and zinc standards. The samples were prepared in an open aluminium crucible (40 μL) outside the DSC apparatus. Measurements were performed in the temperature range from 200 K to 450 K at a constant heating/cooling rate of 10 K min^{-1}. Each measurement at a given temperature was repeated 3 times. For each experiment, a new sample was prepared.

2.5. X-ray diffraction

X-ray diffraction studies were performed using Rigaku Denki D/Max Rapid II diffractometer equipped with a rotating silver anode, an incident beam (002) graphite monochromator and an image plate as a detector in the Debye-Scherrer geometry. The diffraction patterns for neat PVPs, MTZ and PVP-MTZ mixtures were collected 1 day after mixture preparation, at 293 K. The samples were measured in glass capillaries of 1.5 nm diameter. The beam size on the sample was 0.3 mm. The background intensity from the empty capillary was subtracted, and two-dimensional diffraction patterns were converted to the one-dimensional function of the diffraction intensity vs the scattering vector $Q = \frac{4\pi \sin\theta}{\lambda}$, where 2θ is the scattering angle and $\lambda = 0.56$ Å is the wavelength of the incident beam.

2.6. Dynamic light scattering and zeta potential measurements

Hydrodynamic diameters (d_h) and zeta potentials (ZP) of polymer particles were measured on Malvern Zetasizer Nano-ZS (4 mW He—Ne ion laser, $\lambda = 633$ nm) for samples in deionised water (0.5 mg/mL) at 25 °C ± 0.1 °C.

2.7. Transmission electron microscopy

Micelles were visualised by high-resolution transmission electron microscope (TEM, FEI Tecnai G2 Spirit BioTWIN) at 120 kV. The polymer samples in deionised water (0.5 mg/mL) placed on the carbon-coated copper grids (200-mesh) were dried for 2 h.

2.8. UV–Vis spectrophotometry

The measurements by UV–Vis spectrophotometry (Hitachi U-1900) were performed for the samples in methanol. Concentrations of MTZ were calculated based on the calibration curve (please see SI, Fig. S5).

2.9. Critical micellisation concentration

Critical micellisation/aggregation concentrations (CMC/CAC) for all polymers were carried out employing the pendant drop method of surface tension determination on the Kruess DSA 100S goniometer.

3. Results and discussion

Within this work, we selected three different PVP matrices *i)* linear (M_{nSEC} = 66.2 kg/mol; Đ = 1.48) produced via HP thermally-induced free-radical polymerisation, *ii)* unique, four-arm star-shaped PVP (M_{nSEC} = 175.6 kg/mol; Đ = 1.81) synthesised via HP RAFT [28] that was previously not used as potential drug carrier, and *iii)* commercially supplied PVP (commercial name K90; M_{nSEC} = 108.6 kg/mol; Đ = 1.78), which were applied as polymeric support for MTZ. Both synthesised linear and *star*-shaped polymers were characterised by well-defined structural parameters including relatively moderate dispersities, high chain-end fidelity and importantly, high purity, which resulted from the application of metal-free and solvent-free synthetic strategies. On the other hand, the commercial PVP exhibited moderate dispersity and consisted of macromolecular chains of both long and short length probably due to the uncontrolled large-scale synthetic procedure (aqueous solution process in the presence of H_2O_2 as a starter and free metal ions) [37]. The glass transition temperature, T_g, of star-shaped PVP, was significantly lower compared to the linear one (T_g = 429 K vs T_g = 443 K) despite their almost twice higher M_n, which is consistent with other literature data of non-linear polymers (more compactness, lower intrinsic viscosity) [29,38]. Interestingly, higher T_g value (T_g = 450 K) of commercial PVP probably resulted from antiplasticizing effect of the polar solvent used in the polymerisation process that was previously reported by some of us [28] and other researchers [39]. It is hypothesised that both difference in matrices composition/topology and thermodynamic parameters can be attributed to varied ability to drug encapsulation, micellar structure stability, their hydrodynamic diameter values and drug release profiles. Empty (blank) micellar structures and drug-loaded ones were prepared via direct dissolution in an organic solvent (chloroform) following their removal via evaporation with subsequent freeze-drying. It is worth noting that such a preparation pathway was selected as the most suitable for studied herein systems (PVP: metronidazole binary mixtures), among other common methods, including direct dissolution in water or dialysis. Our choice was dictated by the fact that selected herein PVP matrices differed in topology and slightly in composition (the presence of sulfur-based core in star-shaped PVP), which affected their water solubility. In turn, the dialysis method appears to be less advantageous for our systems from the viewpoint of loading a potentially small amount of drug and forming polymer aggregates in the micellization process, which could facilitate the removal of API from self-assembling micelles. Noteworthy, the choice of micellization strategy can significantly influence both the drug encapsulation efficiency and micellar structure parameters (their size and polydispersities). Basically, the latter parameters are affected by the concentration of the polymeric matrix, the nature of the applied organic solvent, and the order of solvents addition. Thus, to investigate the impact of the selected PVP matrix on micelle formation and properties of produced micellar superstructures (empty and drug-loaded), micellization was performed using standardized method (direct dissolution in organic solvent) and constant concentration of polymeric matrix for all systems. In this context it is worth to remind that the same micellization strategy (the solvent evaporation) was already employed for other PVP containing polymeric carriers. [40,41] Although one of the main drawback of this strategy is a necessity of using a toxic solvent; further, NMR and FT-IR analyses of prepared herein formulations clearly indicated that organic solvent has been completely evaporated making this concept acceptable from a biomedical point of view.

Initially, as one of the most significant parameters for the preparation of micellar-based DDS, the critical micellisation/aggregation concentration (CMC/CAC) has been estimated. Note that above CMC/CAC polymeric materials containing amphiphilic domains are expected to arrange in aqueous solutions by self-assembly. Its value can change dramatically with the variation, e.g., in the polymer topology and chain length (through the steric effects) as well as the presence of polar domains (structural effects). Literature data report that the CMC/CAC decreases with the elongation in alkyl chain length, which favours the insoluble domain [42]. This phenomenon can be observed for linear and commercial samples (higher M_n = 108 kg/mol – lower CMC = 0.04 mg/mol) (see Fig. 1). On the other hand, referring to the linear and star-shaped samples obtained via HP solvent-free strategy, the star-like PVP showed lower CMC value (although their M_n is higher than the linear one), which may be an effect of the higher density of PVP segments (compactness) rendering easier the self-assembly process. Therefore, it was found that *star*-like polymers are more prone to form micellar structures and aggregates than linear ones, which is in line with the other literature findings [43].

The resulted micellar and drug-loaded structures were evaluated considering particle sizes, zeta potential (ZP) and drug loading capacity (DLC). We are aware that from the pharmaceutical point of view the most useful/optimal formulations assume a significant excess of the polymeric matrix to the drug. Nevertheless, in our research, apart from the formulation with an excess of the matrix to the MTZ (2:1), we also tested two other systems, i.e., with the lower matrix concentration (1:2) and those with the same concentration of drug and matrix (1:1). In this way, we can get a comprehensive insight into assessing the impact of various formulations on the above-mentioned parameters. Note that similar strategy was also employed in other studies concerning drug-loaded micellar carriers [30–36].

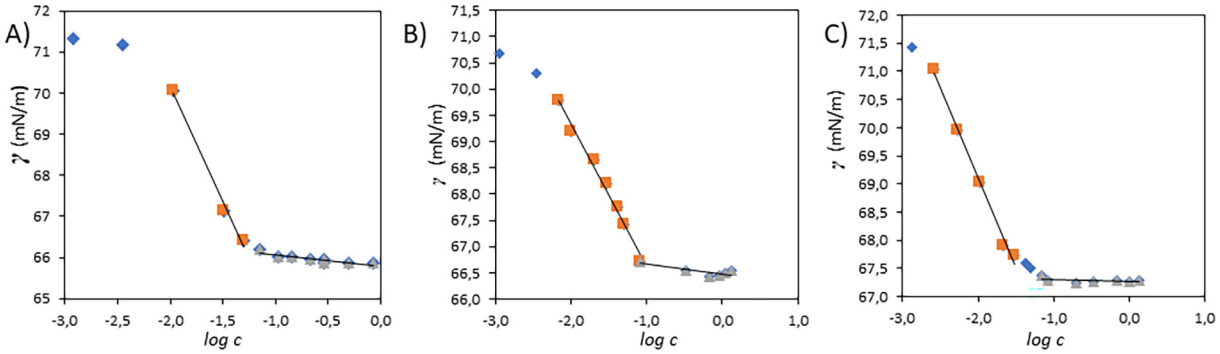

Fig. 1. Determination of CMC/CAC by measuring the surface tension of a serial dilutions A) star PVP (0.05 mg/mL), B) linear PVP (0.10 mg/mL) and C) commercial PVP (0.04 mg/mL). Solid lines are the best linear fits in the two ranges of concentrations. From the change in the slope of γ vs log c, a critical micellisation concentration has been determined.

Table 1
Sizes of micelles (from DLS studies) and ZP of the examined systems.

PVP	Unloaded polymer		2:1 ratio		1:1 ratio		1:2 ratio	
	d_h (nm)	ZP (mV)	d_h (nm)	ZP (mV)	d_h (nm)	ZP (mV)	d_h (nm)	ZP (mV)
star-shaped	16.68	−3.74	23.73	−16.4	21.6	−5.88	14.7	−17.1
linear	29.26	−7.5	14.22	+0.77	14.71	−2.37	14.6	−5.82
commercial	–	–	13.1	−2.13	30.64	−11.3	25.28	−3.5

As presented in Table 1, all micellar structures exhibited relatively small hydrodynamic diameters (d_h) in aqueous solutions. It seemed that star-shaped PVP micelles showed both the smallest size and ZP compared to linear systems, which is a typical phenomenon observed for micelles formed by non-linear macromolecules. After drug encapsulation, the d_h diameters and ZP of DDS have changed significantly. As expected, the weight ratio of PVP to MTZ strongly affects these parameters. The explanation for these results lies in the differences in solubility of both polymeric matrices and the drug as well as the degree of drug dispersion in the PVP matrix. It should be emphasised that the more soluble systems provided more homogenous dispersion of polymers, and thus smaller, more stable micelles. Contrary, in less soluble systems, the micellisation process-induced irregular aggregation of PVP matrices and provided destabilisation of micellar systems. It can also be noted that for all formulations decreasing ZP with increasing MTZ loading suggests weaker stability of the prepared systems (their tendency to aggregation is much higher).

The findings mentioned above also strongly affected the content of the loaded drug. As presented in Fig. 2, at the weight ratio of PVP to drug equal to 1:1, the highest DLC value 76.5% has been noted for linear PVP-based DDS, whereas systems based on star-shaped and commercial PVP revealed similar values of the encapsulated drug (58.5% and 54.5%, respectively). Additionally, for all three systems having higher polymer concentrations (2:1), the lowest DLC values were obtained. Surprisingly, the PVP: MTZ = 1:2 system based on commercial PVP exhibited 90% drug loading (Fig. 2C). However, in this case, drug loading efficiency was the lowest of all the studied systems. It seems that this unexpected scenario resulted from lower water solubility of commercial PVP (at least one of fractions differing in M_n) that was also further reduced by the presence of the polar drug leading to their precipitation. Thus, it can be assumed that the commercial polymer shows little or no suitability for use as a drug carrier.

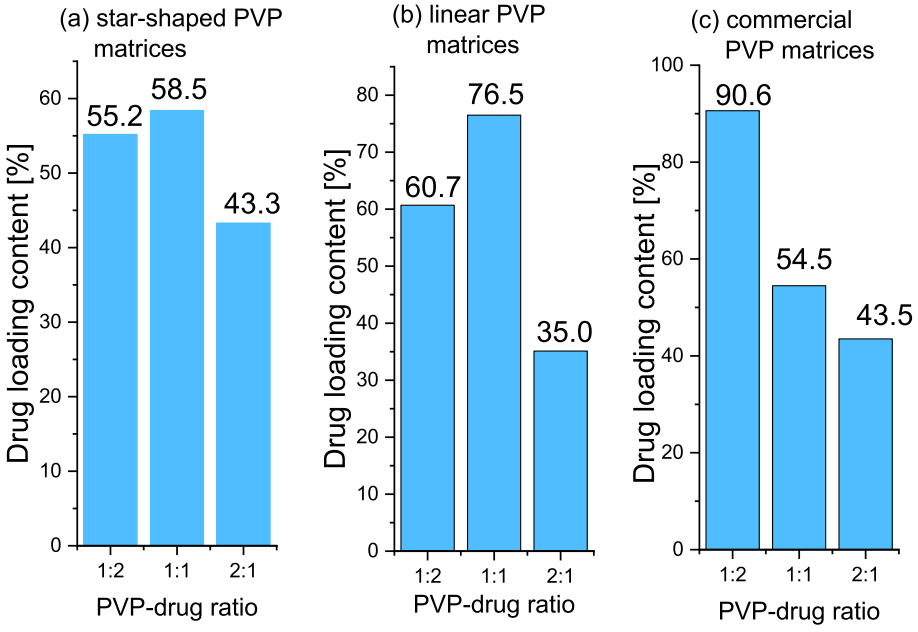

Fig. 2. Drug loading content values for different PVP-MTZ weight ratios for A) *star*-shaped polymer, B) linear polymer and C) commercial polymer.

Within this work, we also visualise the microstructure of the studied DDS using TEM. Interestingly, as it can be seen in Fig. 3, the presence of MTZ seems to force the polymer to self-assembly into spherical micelles. In turn, neat, unloaded PVP polymers form irregular, flocculant aggregates, much smaller than the micelles. Such results might suggest that, at least in the solutions, loaded drug migrates to the core of formed particles and is surrounded by polymer chains. Additionally, linear PVP creates more regular particles than the star-shaped PVP (please compare Fig. 3B vs E). The particles revealed by TEM exhibit larger sizes than those determined by DLS measurements. This discrepancy could be due to the effect of sample preparation for TEM. The evaporation of solvent may drastically increase the concentration of the material and thus cause the aggregation/formation of larger particles. Moreover, such results correspond with the relatively low ZP values suggesting that particles formed in solutions are prone to aggregate when changing/increasing the concentration.

At this point, it needs to be stressed that among all micellar DDS studied herein the most effective for physical entrapment of MTZ are linear one obtained via CRP (PVP:MTZ weight ratio = 1:1) characterised by the lowest hydrodynamic radius of (d_h = 14.7 nm), the highest content of the loaded drug (76.5%) and importantly, the highest stability of produced nanoparticles (ZP = 2.37 mV). Of particular note is that the linear PVP-based DDS has been prepared via HP polymerisation, ensuring the control over polymer (micro)structural parameters (i.e., dispersity, functionality). These systems presented nearly monodisperse structures of polymeric chains that in consequence, allowed for the generation of vehicles of uniform, tuneable and highly stable particles. The implementation of commercial PVP as MTZ carriers yields less-stable nanoparticles (ZP = -11.3 mV) characterised by less regular shapes, probably due to their poorly-defined macromolecular parameters (see Table 1). Besides, their preparation via solvent-assisted methodology could affect the lower DLC value (54.5% at PVP:MTZ weight ratio = 1:1). It is related to the higher content of polar solvent molecules entrapped into polymeric chains. Interestingly, star-shaped matrices also prepared by solvent-free HP CRP methodology were able to encapsulate slightly higher (58.5%) but much lower content of the drug in comparison to the commercial and the linear PVP systems, respectively. DDS composing of star-shaped PVP also showed more stable micellar structures (ZP = -5.88) than those formed by the commercially-supplied PVP.

In the next step, the studied MTZ and obtained polymer-drug mixtures were characterised by DSC to probe their thermal properties as well as phase transitions, see Fig. 4. The heating of the neat crystalline API revealed the presence of one clear endothermic process, melting, occurring at T_m = 436 K, see the inset in Fig. 4A. Nevertheless, it should be mentioned that as the studied MTZ is cooled down, it crystalised at the applied standard cooling rate, 10 K min^{-1}. This indicates that it has an extremely low glass-forming ability, and it cannot

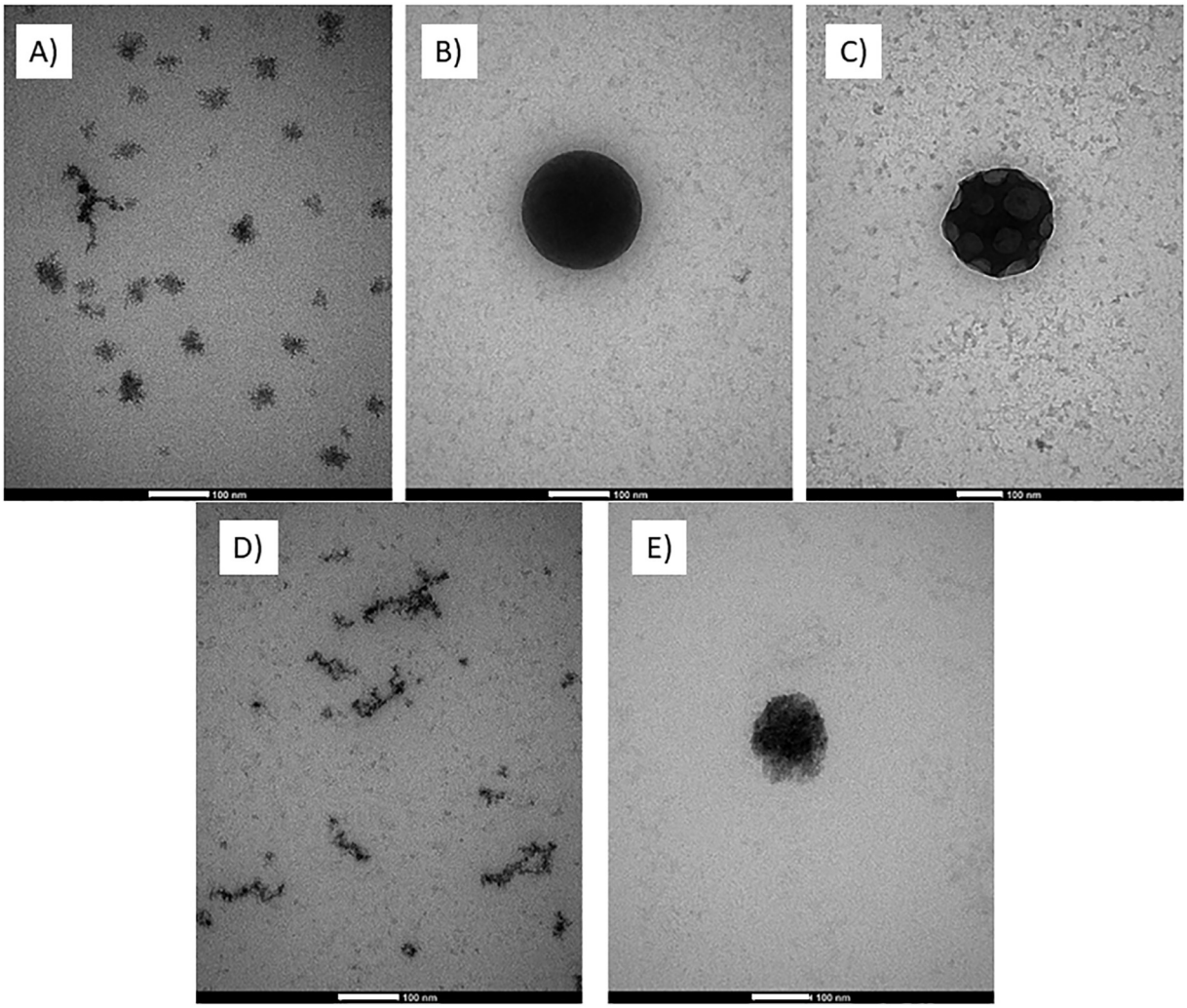

Fig. 3. TEM images of A) unloaded linear PVP, B) linear PVP loaded with MTZ (1:1 ratio), C) degraded micelle of linear PVP loaded with MTZ (1:1 ratio), D) unloaded star-shaped PVP and E) star-shaped PVP loaded with MTZ (1:1 ratio). Bar = 100 nm.

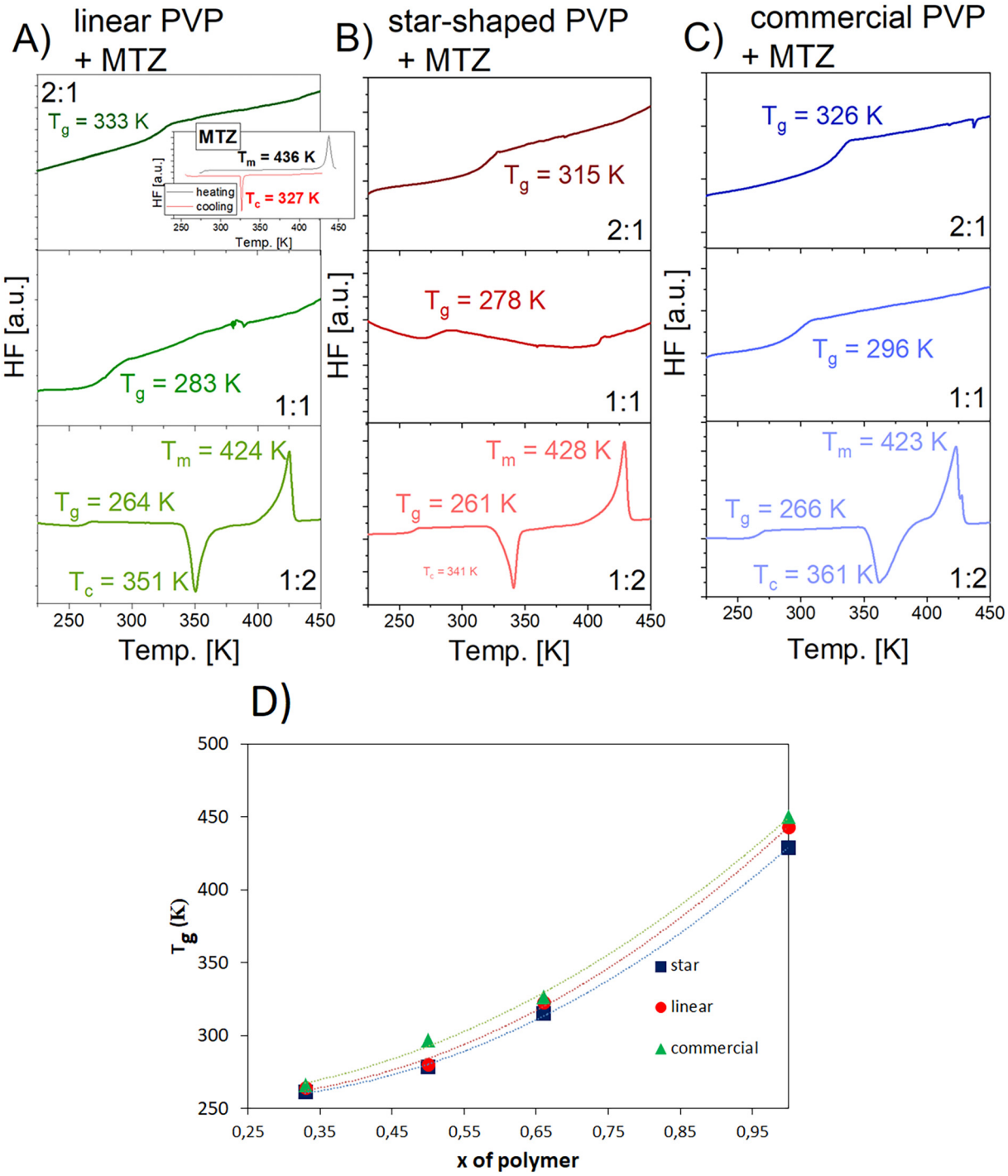

Fig. 4. A-C) DSC thermograms of the studied polymer-drug mixtures for A) linear, B) star-shaped and C) commercial PVPs. As the inset in A), DSC thermogram of the neat MTZ is presented. Heating/cooling rate of performed DSC measurements was equal to 10 K min^{-1}. D) T_g vs weigh a fraction of PVP (x) in the indicated micellar formulations.

be supercooled and does not vitrify. Interestingly, DSC curves recorded for the various polymer-drug mixtures revealed a significantly different behaviour when compared to the neat MTZ. As observed, all thermograms measured for the examined mixtures exhibit the presence of a clear heat capacity jumps at low temperatures, related to the glass transition phenomenon, independently to the applied kind of PVP formulations, see Fig. 4.

Interestingly, T_gs of all types of binary systems are much lower with respect to neat amorphous PVP, which is characterised by a high T_g (see Fig. 4D and Table S1 in the SI). As previously mentioned, T_g of linear, *star*-shaped and commercial polymers are $T_g = 443$ K, $T_g = 429$ K and $T_g = 450$ K, respectively. The glass transition temperature of the studied PVP-API mixture differs significantly with MTZ concentration, where a strong decrease of T_g of the studied micellar systems indicates a strong plasticising effect of a drug on the glass transition temperature in binary systems, see Fig. 4D. It can be clearly seen that for mixtures with high MTZ content, the influence is very strong, (T_g lower by more than 100 K). On the other hand, in the case of 1:2 polymer-drug mixtures, the additional exothermal event related to the crystallisation process, followed by a clear melting, can be observed. Obtained data indicated

that MTZ dispersed in the polymer matrix (1:2 weight ratio) is the least physically stable and tends to crystallise upon heating. Nevertheless, it should be pointed out that the determined values of T_m of MTZ in the studied micellar systems are comparable independently to the applied PVP formulation and are significantly lower when compared to the neat crystalline API, see the inset in Fig. 4A. One can recall that usually in the case of binary systems, the decrease of the melting temperature is often discussed in terms of either strong intermolecular interactions between both components, size of crystallites, or the presence of various polymorphic forms of API obtained at given conditions.

To verify this hypothesis, we have performed further XRD measurements on the produced micelles after approximately one week of storage. As it is shown in Fig. 5A, diffraction patterns for neat PVPs display broad peaks, typical for amorphous-like structure with no long-range order. In turn, the sample of commercial MTZ gives diffraction pattern with Bragg peaks, characteristic for crystalline material. The crystal system of commercial MTZ was identified as monoclinic P 21/c space group with lattice parameters a ≈ 7.03, b ≈ 8.73, b ≈ 12. 82 Å and cell angles α ≈ 90, β ≈ 94.5, γ ≈ 90° (CCDC number 1212679 in Cambridge Crystallographic Data Centre). In case of all polymer-drug mixtures in 1:2 ratio, one can see that the diffraction patterns are composed of contribution from non-crystalline PVP and crystalline MTZ in the same polymorphic form as the commercial reference drug. Moreover, for other mixtures with higher concentrations of polymer (1:1 and 2:1), we also observed the crystallisation of MTZ to the same crystal phase (see Fig. S2 in the SI). The size of crystallites in the direction perpendicular to the (011) lattice plane, $D_{(011)}$, calculated for the commercial MTZ using the Scherrer formula [35] ($L = K\lambda/FWHM\cos\theta$, where the Scherrer constant K was equal to 0.9, θ is the Bragg angle of the (011) reflection at around 0.9 $Å^{-1}$ and FWHM is its full-width at half-maximum) was 12 ± 1 nm. The widths of Bragg peaks for MTZ in the mixtures, determined from the diffractograms after subtraction of the contribution from PVP, are very similar to that determined for the neat drug. Therefore, we can suppose that the sizes of MTZ crystallites in the mixtures are also on the order of 12 nm. We did not observe any trend in the behaviour of crystallite size depending on the type and amount of PVP.

Herein, it can be emphasised that the XRD data showing partial or full crystallisation of MTZ in micellar systems stay at first sight in contrast to the DSC thermograms, which demonstrated that the studied systems were amorphous just after preparation. To justify these results, one can consider that in the systems of lower PVP concentration, there could be some residual API nuclei, which dissolved in PVP upon heating in DSC aluminium pans. Therefore, we observed only glass transition peak on DSC curves and did not detect any signal coming from the heat of fusion of crystalline API. A better understanding of the discrepancy between results from XRD and DSC brought additional diffraction measurements just after the preparation of the PVP-MTZ systems. In Fig. 5B one can clearly see that in the micelles measured 1 h after preparation the degree of crystallinity is much lower and the content of MTZ in the amorphous form is higher than in the sample measured one week after preparation. It suggests that even though produced micellar systems are completely or partially amorphous just after the preparation, this state is not stable and MTZ tends to recrystallise very quickly to the same polymorphic form and size of crystallites as the original reference API. Having this result in mind, one can claim that the strong depression of the T_g in binary mixtures as well as T_m of MTZ is due to strong molecular interactions between API and polymer irrespectively on the source and topology.

As a final point of our investigations, we performed drug release studies for each considered herein system. As the most optimal, a dialysis method has been chosen for this purpose. Solutions of the obtained polymer-drug mixtures (c = 2 mg/mL) were placed into the dialysis membrane bags and then immersed into the PBS pH = 7,4 at 310 K

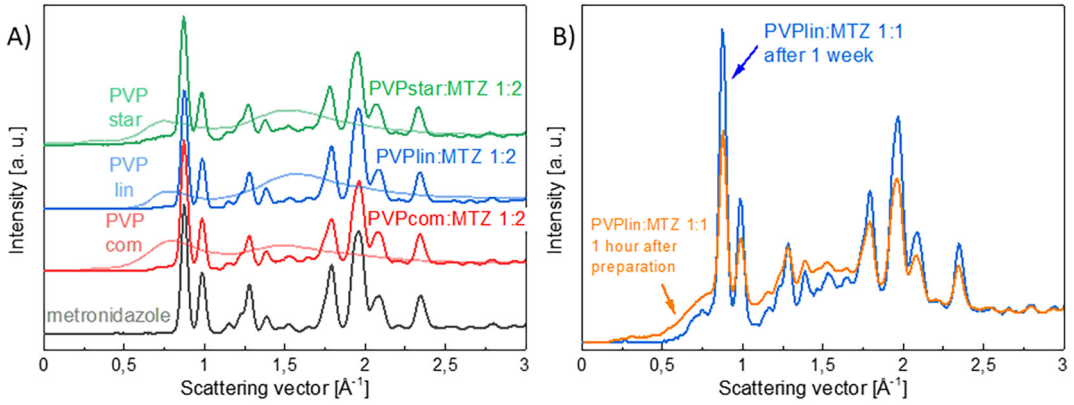

Fig. 5. A) XRD patterns of the studied neat MTZ, PVP polymers and polymer-drug mixtures in 1:2 weight ratio. B) XRD patterns of the PVP-MTZ mixture in 1:1 weight ratio measured just after the sample preparation and after 1 week of storage.

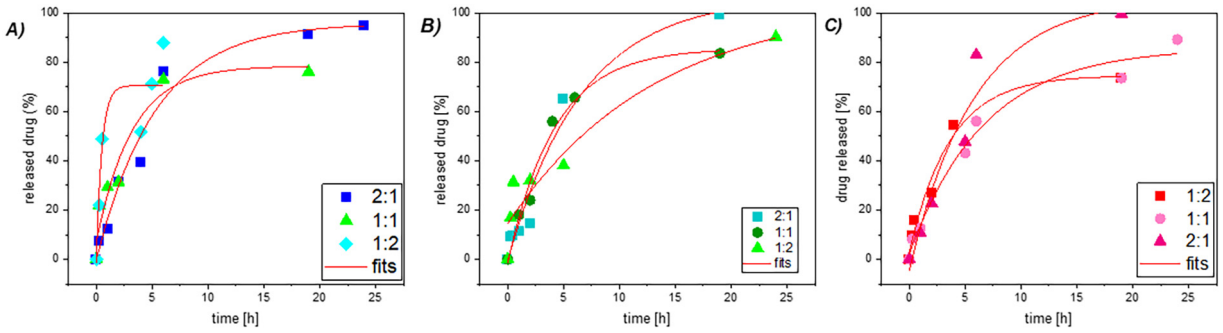

Fig. 6. Drug release profiles for three PVP-MTZ systems with different polymer-drug ratios. A) Star-shaped PVP, B) linear PVP and C) commercial PVP.

what imitates the physiological conditions. Samples were taken in time, and the obtained results were collected in Fig. 6.

All samples exhibited a burst release of MTZ in the first 5 h of the experiment. After this time, the release slows down and reaches up to 90% in the 30 h, irrespectively of the type of the applied polymer. A clear dependency of release speed on the concentration of MTZ in the polymer matrix was shown. All systems exhibited much faster drug release as MTZ concentration in the polymer matrix increased. For the star-shaped system of 1:2 PVPMTZ ratio, which released more than 90% of the drug within 6 h, this relationship is exceptionally clear. Additionally, the mathematical models were fitted to the release process (see the SI, Fig. S3, Table S2). As expected, none of the tested samples followed the zero-order model. The model that turned out to describe the results in the best way was the first-order (I^{st}) approach, which would indicate that the release of MTZ from the investigated systems is concentration-dependent to the greatest extent. For some of the proposed mixtures, we additionally found a good correlation with the Higuchi model, what might suggest that the diffusion process also clearly influences the release of MTZ. Similar results were obtained for various delivery systems designed for this drug [14,44], [45]. Taking advantage of fitting dissolution curves to the I^{st} order kinetics, we have also determined drug release rate constants. The dependence of this constant on the PVP concentration in the micellar system was presented (see the SI, Fig. S4). As it turned out, these results also confirmed that the *star*-shaped topology influences significantly the MTZ release rate from the polymer matrix. For both linear and commercial PVP, the release constants were basically the same. These findings lead to the conclusion that linear topology of PVP is better suited for sustained drug release from micellar systems than the star-shaped one. Systems with lower MTZ content (both 1:1 and 2:1 polymer-drug ratio) showed no significant differences in drug release.

4. Conclusions

New PVP-based DDS produced via different synthetic strategy (controlled vs uncontrolled polymerisation) varying in topology, and chain lengths have been designed for MTZ. After solubilisation on the aqueous medium, PVP-MTZ mixtures formed micellar structures, what was confirmed by TEM analysis. It is worth noting that the micellisation was induced by the presence of the drug, and was not observed for neat polymers. Both very low ZP and low CMC values suggest that the obtained systems are prone to aggregation due to the concentration changes. This would be a great explanation of discrepancies in sizes of matrices hydrodynamic diameters values. Among all micellar systems explored herein, the linear-based PVP DDS produced via CRP methodology showed the most promising features as MTZ nanocarriers. It has also been shown that mixing of MTZ with PVP significantly reduces the glass transition temperature of the binary mixture (more than 100 K).

Designed herein, DDS could release MTZ more than 6 h. Our studies revealed that the burst release effect occurs for all proposed systems, resulting in the initial release of about 60% of the drug in first 5 h, independently of the type of PVP polymer applied. The concentration of the micellar system in the aqueous medium and diffusion have been shown as the main factors influencing the release process. It is anticipated that results presented herein will advanced design and development of novel PVP-based DDS of MTZ.

Declaration of Competing Interest

None.

Acknowledgements

K.K., M.T., R.B., P.M., and R.B. are thankful for financial support from the National Centre for Research and Development within POIR.04.01.04-00-0142/17.

Appendix A. Supplementary data

Supplementary data to this article can be found online at https://doi.org/10.1016/j.molliq.2021.115789.

References

[1] O. Pillai, R. Panchagnula, Polymers in drug delivery Omathanu Pillai and Ramesh Panchagnula, Curr. Opin. Chem. Biol. 5 (2001) 447–451.
[2] W.B. Liechty, D.R. Kryscio, B.V. Slaughter, N.A. Peppas, Polymers for drug delivery systems, Annu. Rev. Chem. Biomol. Eng. 1 (2010) 149–173, https://doi.org/10.1146/annurev-chembioeng-073009-100847.
[3] I.R. Calori, G. Braga, P. da C.C. de Jesus, H. Bi, A.C. Tedesco, Polymer scaffolds as drug delivery systems, Eur. Polym. J. 129 (2020), 109621, https://doi.org/10.1016/j.eurpolymj.2020.109621.
[4] R.B. Chavan, R. Thipparaboina, D. Kumar, N.R. Shastri, Evaluation of the inhibitory potential of HPMC, PVP and HPC polymers on nucleation and crystal growth, RSC Adv. 6 (2016) 77569–77576, https://doi.org/10.1039/c6ra19746a.
[5] Z. Ahmad, A. Shah, M. Siddiq, H.B. Kraatz, Polymeric micelles as drug delivery vehicles, RSC Adv. 4 (2014) 17028–17038, https://doi.org/10.1039/c3ra47370h.
[6] M. Śmiga-Matuszowicz, K. Jaszcz, J. Lukaszczyk, M. Kaczmarek, M. Lesiak, A.L. Sieroń, M. Staszuk, R. Pilawka, M. Mierzwiński, D. Kusz, Characterization of polysuccinate and hydroxyapatite-based nanocomposites containing poly(ester-anhydride) microspheres, Polym. Adv. Technol. 25 (2014) 1145–1154, https://doi.org/10.1002/pat.3368.
[7] R. Laitinen, K. Lobmann, C.J. Strachan, H. Grohganz, T. Rades, Emerging trends in the stabilization of amorphous drugs, Int. J. Pharm. 453 (2013) 65–79, https://doi.org/10.1016/j.ijpharm.2012.04.066.
[8] J.L. Arias, G.I. Martinez-Soler, M. Lopez-Viota, A. Ruiz Martinez, Formulation of chitosan nanoparticles loaded with metronidazole for the treatment of infectious diseases, Lett. Drug Des. Discov. 7 (2010) 70–78.
[9] K. Czarnobaj, Sol-gel-processed silica/polydimethylsiloxane/calcium xerogels as polymeric matrices for metronidazole delivery system, Polym. Bull. 66 (2011) 223–237, https://doi.org/10.1007/s00289-010-0332-8.
[10] A. Bani-Jaber, L. Al-Aani, H. Alkhatib, B. Al-Khalidi, Prolonged intragastric drug delivery mediated by eudragit® E-carrageenan polyelectrolyte matrix tablets, AAPS PharmSciTech 12 (2011) 354–361, https://doi.org/10.1208/s12249-011-9595-0.
[11] D.S. Jones, G.P. Andrews, D.L. Caldwell, C. Lorimer, S.P. Gorman, C.P. McCoy, Novel semi-interpenetrating hydrogel networks with enhanced mechanical properties and thermoresponsive engineered drug delivery, designed as bioactive endotracheal tube biomaterials, Eur. J. Pharm. Biopharm. 82 (2012) 563–571, https://doi.org/10.1016/j.ejpb.2012.07.019.
[12] F. Bian, L. Jia, W. Yu, M. Liu, Self-assembled micelles of N-phthaloylchitosan-g-polyvinylpyrrolidone for drug delivery, Carbohydr. Polym. 76 (2009) 454–459, https://doi.org/10.1016/j.carbpol.2008.11.008.
[13] M. Szekalska, K. Winnicka, A. Czajkowska-Kośnik, K. Sosnowska, A. Amelian, Evaluation of alginate microspheres with metronidazole obtained by the spray drying technique, Acta Pol. Pharm. Drug Res. 72 (2015) 569–578.
[14] L. Nohemann, M.P. de Almeida, P.C. Ferrari, Floating ability and drug release evaluation of gastroretentive microparticles system containing metronidazole obtained by spray drying, Brazil. J. Pharm. Sci. 53 (2017) 1–13, https://doi.org/10.1590/s2175-97902017000115218.
[15] E.G. Pehlivan, Y. Ek, D. Topkaya, U.H. Tazebay, F. Dumoulin, Effect of PVP formulation on the in vitro photodynamic efficiency of a photosensitizing phthalocyanine, J. Porphyrins Phthalocyanines 23 (2019) 1587–1591, https://doi.org/10.1142/S108842461950189X.
[16] M. Rasekh, C. Karavasili, Y.L. Soong, N. Bouropoulos, M. Morris, D. Armitage, X. Li, D.G. Fatouros, Z. Ahmad, Electrospun PVP-indomethacin constituents for transdermal dressings and drug delivery devices, Int. J. Pharm. 473 (2014) 95–104, https://doi.org/10.1016/j.ijpharm.2014.06.059.
[17] S. Tort, A. Yıldız, F. Tuğcu-Demiröz, G. Akca, Ö. Kuzukıran, F. Acartürk, Development and characterization of rapid dissolving ornidazole loaded PVP electrospun fibers, Pharm. Dev. Technol. 24 (2019) 864–873, https://doi.org/10.1080/10837450.2019.1615088.
[18] H. Lee, G. Xu, D. Kharaghani, M. Nishino, K.H. Song, J.S. Lee, I.S. Kim, Electrospun trilayered zein/PVP-GO/zein nanofiber mats for providing biphasic drug release profiles, Int. J. Pharm. 531 (2017) 101–107, https://doi.org/10.1016/j.ijpharm.2017.08.081.
[19] A.N. Zelikin, G.K. Such, A. Postma, F. Caruso, Poly(vinylpyrrolidone) for bioconjugation and surface ligand immobilization, Biomacromolecules. 8 (2007) 2950–2953, https://doi.org/10.1021/bm700498j.
[20] P.W. Reader, R. Pfukwa, S. Jokonya, G.E. Arnott, B. Klumperman, Synthesis of α,ω-heterotelechelic PVP for bioconjugation: Via a one-pot orthogonal end-group modification procedure, Polym. Chem. 7 (2016) 6450–6456, https://doi.org/10.1039/c6py01296e.
[21] Y. Kaneda, Y. Tsutsumi, Y. Yoshioka, H. Kamada, Y. Yamamoto, H. Kodaira, S.I. Tsunoda, T. Okamoto, Y. Mukai, H. Shibata, S. Nakagawa, T. Mayumi, The use of PVP as a polymeric carrier to improve the plasma half-life of drugs, Biomaterials. 25 (2004) 3259–3266, https://doi.org/10.1016/j.biomaterials.2003.10.003.
[22] V. Prosapio, I. De Marco, M. Scognamiglio, E. Reverchon, Folic acid-PVP nanostructured composite microparticles by supercritical antisolvent precipitation, Chem. Eng. J. 277 (2015) 286–294, https://doi.org/10.1016/j.cej.2015.04.149.
[23] R.H. Sizílio, J.G. Galvão, G.G.G. Trindade, L.T.S. Pina, L.N. Andrade, J.K.M.C. Gonsalves, A.A.M. Lira, M.V. Chaud, T.F.R. Alves, M.L.P.M. Arguelho, R.S. Nunes, Chitosan/pvp-

based mucoadhesive membranes as a promising delivery system of betamethasone-17-valerate for aphthous stomatitis, Carbohydr. Polym. 190 (2018) 339–345, https://doi.org/10.1016/j.carbpol.2018.02.079.
[24] R.K. Mishra, M. Datt, A.K. Banthia, Synthesis and characterization of pectin/pvp hydrogel membranes for drug delivery system, AAPS PharmSciTech 9 (2008) 395–403, https://doi.org/10.1208/s12249-008-9048-6.
[25] L. McDowall, G. Chen, M.H. Stenzel, Synthesis of seven-arm poly(vinyl pyrrolidone) star polymers with lysozyme core prepared by MADIX/RAFT polymerization, Macromol. Rapid Commun. 29 (2008) 1666–1671, https://doi.org/10.1002/marc.200800416.
[26] R. Devasia, R.L. Bindu, R. Borsali, N. Mougin, Y. Gnanou, Controlled radical polymerization of N-vinylpyrrolidone by reversible addition-fragmentation chain transfer process, Macromol. Symp. 229 (2005) 8–17, https://doi.org/10.1002/masy.200551102.
[27] M. Tarnacka, P. Maksym, A. Zięba, A. Mielańczyk, M. Geppert-Rybczyńska, L. Leon-Boigues, C. Mijangos, K. Kamiński, M. Paluch, The application of spatially restricted geometries as a unique route to produce well-defined poly(vinyl pyrrolidones) via free radical polymerisation, Chem. Commun. 55 (2019) 6441–6444, https://doi.org/10.1039/c9cc02625h.
[28] P. Maksym, M. Tarnacka, D. Heczko, J. Knapik-Kowalczuk, A. Mielańczyk, R. Bernat, G. Garbacz, K. Kaminski, M. Paluch, Pressure-assisted solvent- and catalyst-free production of well-defined poly(1-vinyl-2-pyrrolidone) for biomedical applications, RSC Adv. 10 (2020) 21593–21601, https://doi.org/10.1039/d0ra02246b.
[29] P. Maksym, M. Tarnacka, R. Bernat, R. Bielas, B. Hachuła, K. Kamiński, M. Paluch, Pressure-assisted strategy for the synthesis of vinyl pyrrolidone-based macro-star photoiniferters. A route to star block copolymers, J. Polym. Sci. 58 (2020) 1393–1399, https://doi.org/10.1002/pol.20200037.
[30] S. Tivari, P. Verma, Microencapsulation technique by solvent evaporation method (study of effect of process variables), Int. J. Pharm. Life Sci. 2 (2011) 998–1005.
[31] D. Neugebauer, J. Odrobińska, R. Bielas, A. Mielańczyk, Design of systems based on 4-armed star-shaped polyacids for indomethacin delivery, New J. Chem. 40 (2016) 10002–10011, https://doi.org/10.1039/c6nj02346k.
[32] A. Mielańczyk, J. Odrobińska, S. Grządka, Ł. Mielańczyk, D. Neugebauer, Miktoarm star copolymers from D-(−)-salicin core aggregated into dandelion-like structures as anticancer drug delivery systems: synthesis, self-assembly and drug release, Int. J. Pharm. 515 (2016) 515–526, https://doi.org/10.1016/j.ijpharm.2016.10.034.
[33] J. Odrobińska, K. Niesyto, K. Erfurt, A. Siewniak, A. Mielańczyk, D. Neugebauer, Retinol-containing graft copolymers for delivery of skin-curing agents, Pharmaceutics. 11 (2019) 18–20, https://doi.org/10.3390/pharmaceutics11080378.
[34] J. Odrobińska, L. Mielańczyk, D. Neugebauer, 4-N-butylresorcinol-based linear and graft polymethacrylates for arbutin and vitamins delivery by micellar systems, Polymers (Basel). 12 (2020)https://doi.org/10.3390/polym12020330.
[35] J. Odrobińska, M. Skonieczna, D. Neugebauer, PEG graft polymer carriers of antioxidants: in vitro evaluation for transdermal delivery, Pharmaceutics. 12 (2020) 1–16, https://doi.org/10.3390/pharmaceutics12121178.
[36] J. Odrobińska, D. Neugebauer, Retinol derivative as bioinitiator in the synthesis of hydroxyl-functionalized polymethacrylates for micellar delivery systems, Express Polym Lett 13 (2019) 806–817, https://doi.org/10.3144/expresspolymlett.2019.69.
[37] A. Nuber, S. Lang, A. Sanner, G. Schroeder, Preparation of Polyvinylpyrrolidone, US4786699A, 1988.
[38] Y.L. Zhao, Q. Cai, J. Jiang, X.T. Shuai, J.Z. Bei, C.F. Chen, F. Xi, Synthesis and thermal properties of novel star-shaped poly(L-lactide)s with starburst PAMAM-OH dendrimer macroinitiator, Polymer (Guildf). 43 (2002) 5819–5825, https://doi.org/10.1016/S0032-3861(02)00529-3.
[39] F. Haaf, A. Sanner, F. Straub, Polymers of n-vinylpyrrolidone: synthesis, characterization and uses, Polym. J. 17 (1985) 143–152, https://doi.org/10.1295/polymj.17.143.
[40] N.M. Ranjha, I.U. Khan, S. Naseem, Encapsulation and characterization of flurbiprofen loaded poly(ε-caprolactone)-poly(vinylpyrrolidone) blend micropheres by solvent evaporation method, J. Sol-Gel Sci. Technol. 50 (2009) 281–289, https://doi.org/10.1007/s10971-009-1957-7.
[41] C. Perez, A. Sanchez, D. Putnam, D. Ting, R. Langer, M.J. Alonso, Poly(lactic acid)-poly (ethylene glycol) nanoparticles as new carriers for the delivery of plasmid DNA, J. Control. Release 75 (2001) 211–224, https://doi.org/10.1016/S0168-3659(01)00397-2.
[42] B. Lindman, Physico-chemical properties of surfactants, in: K. Holmberg (Ed.), Handb. Appl. Surf. Colloid Chem, John Wiley & Sons, Ltd, New York, NY 2001, pp. 421–444.
[43] C. Allen, D. Maysinger, A. Eisenberg, Nano-engineering block copolymer aggregates for drug delivery, Colloids Surf. B: Biointerfaces 16 (1999) 3–27.
[44] C.F. Vechci, R.S. dos Santos, M.L. Bruschi, Technological development of mucoadhesive film containing poloxamer 407, polyvinyl alcohol and polyvinylpyrrolidone for buccal metronidazole delivery, Ther. Deliv. 11 (2020) 431–446.
[45] M.A.C. da Silva, R.N. Oliveira, R.H. Mendonça, T.G.B. Lourenço, A.P.V. Colombo, M.N. Tanaka, E.M.O. Tude, M.F. da Costa, R.M.S.M. Thiré, Evaluation of metronidazole-loaded poly(3-hydroxybutyrate) membranes to potential application in periodontitis treatment, J. Biomed. Mater. Res. Part B Appl. Biomater. 104 (2016) 106–115.